

trates the feasibility of extending FDISH bandwidth at least 5-fold. Signal level, currently limited by strong WLC chirp, will be improved $\sim 1000\times$ by compressing the selected WLC. In addition, fringe contrast, currently limited by mismatched amplitudes of the two interfering signals at some wavelengths, will be improved by shaping the reference spectrum.

1. R.K. Chang *et al.*, "Relative phase measurement between fundamental and second-harmonic light", *Phys. Rev. Lett.* 15, 6-8 (1965); R. Stolle *et al.*, "Phase measurements in nonlinear optics", *Appl. Phys. B* 63, 491-498 (1996).
2. P.T. Wilson *et al.*, "Frequency-domain interferometric second-harmonic spectroscopy", *Opt. Lett.* 24, 496-498 (1999).
3. J.I. Dadap *et al.*, "Femtosecond carrier-induced screening of DC electric-field-induced second-harmonic generation at the Si(001)-SiO₂ interface", *Opt. Lett.* 22, 901-903 (1997); O.A. Aktsipetrov *et al.*, "dc-electric-field-induced second-harmonic generation in Si(111)-SiO₂-Cr metal-oxide-semiconductor structures", *Phys. Rev. B* 54, 1825-1832 (1996).
4. J.K. Ranka *et al.*, "Visible continuum generation in air-silica microstructure optical fibers with anomalous dispersion at 800 nm", *Opt. Lett.* 25, 25-27 (2000).
5. D.R. Yankelevich *et al.*, "Molecular engineering of polymer films for amplitude and phase measurements of Ti:sapphire femtosecond pulses", *Opt. Lett.* 21, 1487-1489 (1996).

CThD5

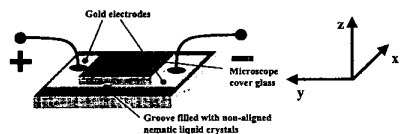
9:00 am

3-dimensional Electric Field Visualization Utilizing Electric-field-Induced-second Harmonic-generation in Liquid Crystals

Shi-Wei Chu, Francois Bresson, I-Hsiu Chen, Jin-Wei Shi, Ming-Chun Tien, and Chi-Kuang Sun, Graduate Institute of Electro-Optical Engineering, National Taiwan University, Taipei, TAIWAN, 10617 R.O.C., Email: r8941009@ee.ntu.edu.tw.

F.E. Hernandez, School of Optics/CREOL, University of Central Florida Orlando, FL 32816-2700, Email: feha@mail.creol.ucf.edu

As a result of the wide use of electronic and optoelectronics devices, the need for efficient tool to characterize integrated circuits (IC) is growing up. Electron-beam-based test systems are widely used but require heavy work and technical effort. Thus it is beneficial to find out alternative easier ways for mapping electric field. Pockels effect has been used effectively to probe electric field in circuits.¹ Utilizing electric-field-induced-second-

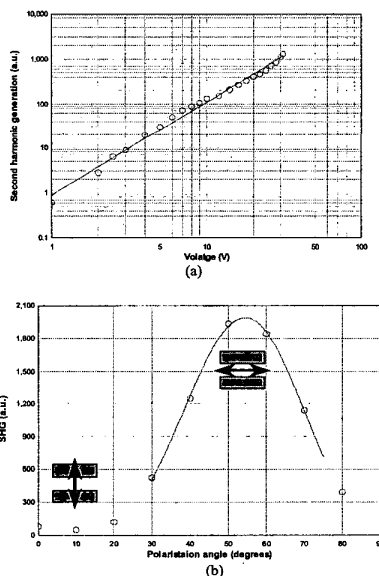


CThD5 Fig. 1. The integrated circuit like sample. The width of the groove between the electrodes is 10 μm .

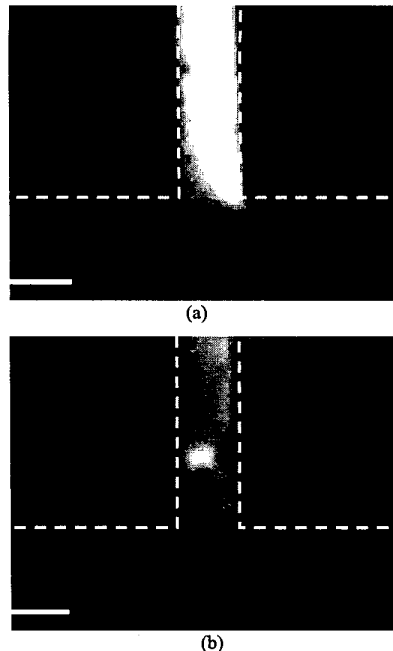
harmonic-generation (EFISHG) to probe electric field intensity has been studied recently.²⁻⁵ EFISHG measurement shows some advantages over EO sampling technique. The detection of EFISHG signal is easier than that of pockels effect. The dependence of the polarization in EFISHG measurement is helpful in making a mapping of the electric field vector. In addition, EFISHG measurement has the characteristic of background free and present no principle limitation from 0 to the breakdown voltage. Here we demonstrate a 3-dimensional electric-field visualization utilizing EFISHG effect in nematic liquid crystals. The visualization was easily achieved with a second-harmonic-generation (SHG) confocal microscope with high spatial resolution on the order of or less than 1 μm .

Figure 1 shows an example of the test samples we used. Two gold electrodes were plated on glass slide with a 10 μm wide and 0.5 μm deep gap between them. Liquid crystals filled the gap and formed a thin layer between the sample and the cover glass. We used a SHG microscope driven by a femtosecond Cr:forsterite laser at 1230 nm. Its spatial resolution, which is mainly dependent on the objective we used, was better than 0.8 μm in xy plane and 1.6 μm in z direction respectively.

Figure 2(a) shows a typical EFISHG response versus applied voltage in nematic liquid crystal. The slope of data fitting line is 1.98, showing the square dependence as expected in EFISHG. Figure 2 (b) shows the dependence of EFISHG intensity and the polarization of the pump. As



CThD5 Fig. 2. (a) EFISHG response versus applied voltage in nematic liquid crystal in log-log scale. The dots are the experimental data. The line is a linear approximation by least square method. (b) EFISHG response versus pump polarization. The angle represent the rotation of the half wave plate, the actual rotation of the polarization is twice. The origine is arbitrary. The maximum occurs when the pump field (symbolized by the double arrow) is perpendicular to the electric field generated by the electrodes (symbolized by the rectangles).



CThD5 Fig. 3. EFISHG xy-images (a) at the depth of the gold electrodes and (b) at the height 5 μm above (a). Dash lines: edge of electrode. Scale bar: 10 μm .

shown by the small drawings, the maximum is reached when the polarization of the pump (symbolized by the double array) is perpendicular to the static electric field (the two rectangles symbolize the electrodes). The result is a cosine response. Also, there was no SHG observed before the static electric field was applied, which showed the background free characteristic of this method.

Figure 3 shows an example of the EFISHG xy-images taken from a CCD in the scanning SHG microscope on the test sample shown in Figure 1. The incident direction of the laser was along the z-axis in figure 1. The polarization of the laser was along the gap that was perpendicular to the electric field. The two images with the same intensity scales show the difference of electric field in different z positions. Figure 3 (a) was taken at the plain of the electrodes, while figure 3 (b) was taken at 5 μm higher than (a). With the great sectioning power in confocal microscope, 3D images can be easily obtained combining different height images. More data will be presented including 3D images.

1. K.J. Weingarten *et al.* "Picosecond optical sampling of GaAs integrated circuit," *IEEE J. Quantum Electron.* 24, 198-220 (1998).
2. C. Ohlhoff *et al.* "Optical second-harmonic probe for silicon millimeter-wave circuits," *Appl. Phys. Lett.* 68, 12, 1699-1701 (1996).
3. J.D. Canterbury, P.T. Wilson, and M.C. Downer "Electric-field-induced second-harmonic-generation microscopy," in *the Proceedings of CLEO/QELS 2000*, 218 (2000).
4. C.K. Sun, and S.W. Chu *et al.* "Scanning second-harmonic/third-harmonic generation microscopy of gallium nitride," *Appl. Phys. Lett.* 77, 15, 2331 (2000).

5. R. Macdonald *et al.*, "Antiferroelectricity and chiral order in new liquid crystals of nonchiral molecules studied by optical second harmonic generation", *Phys. Rev. Lett.*, 81, 4408-4411 (1998).

CThD6

9:15 am

Application of Second-harmonic Generation Combined with the Electro-optic Effect for Electrical Field Measurements

Nilesh J. Vasa, Masao Yoshioka, Shigeru Yokoyama, Interdisciplinary Graduate School of Engineering Sciences, Kyushu University, Fukuoka 816-8580, Japan, Email: vasa@ence.kyushu-u.ac.jp

Mitsuo Maeda, Graduate School of I.S.E.E., Kyushu University, Fukuoka 812-8581, Japan

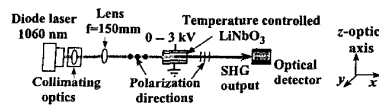
Hirohito Takeshita, Michitaka Nakahara, Kyushu Electric Power Co., Inc., Fukuoka 810-8720, Japan

Optical electric field and voltage sensors are of considerable interest to the electric power industry. Their advantages compared with those of traditional instrument transformers include immunity to electromagnetic interference, response to changes in electric field in the frequency range from dc to GHz, and so on. Commonly, these sensors utilize the electro-optic effect (Pockels effect) in electro-optic crystals.¹

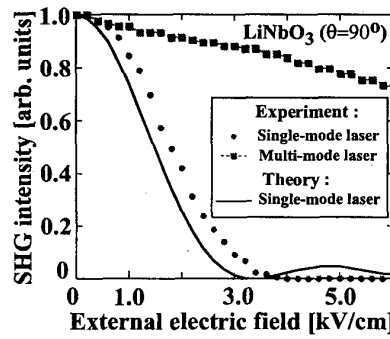
Here, a novel approach of measuring the electric field is proposed by combining second-harmonic generation (SHG) with the electro-optic effect.^{2,3} In SHG with an electro-optic crystal, when the interacting pump and the SHG wave satisfies the phase matching condition, the SHG output can be obtained. However, when an external electric field is applied, the refractive indices alters due to electro-optic effect and the phase matched condition changes resulting in the output variation which can be used for the measurement of the electric field. The advantages compared with the Pockels sensors are: (1) direct measurement of the SHG output results in higher signal to noise ratio; (2) phase matching conditions can easily be offset to monitor higher electric fields; (3) compact fiber coupled assemblies without waveplates, analyzers are possible. In the present work, a diode laser is used with a nonlinear, electro-optic crystal and the feasibility of SHG for the electric field measurement is studied.

Figure 1 shows the experimental setup. In the experiment, the collimated output of the diode laser (≈ 1060 nm) was focused into a LiNbO₃ crystal ($5 \times 5 \times 13$ mm long) for the noncritical phase matched ($\theta = 90^\circ$) SHG output. The phase matching condition was adjusted by temperature control ($\approx 63^\circ\text{C}$), such that a maximum SHG output was attained when the external electric field was zero.

Figure 2 shows the variation in the SHG out-



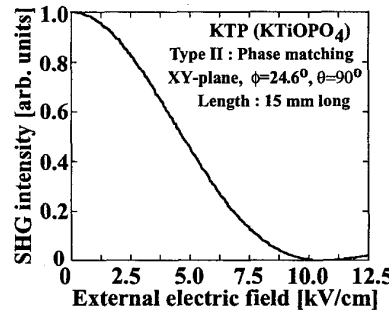
CThD6 Fig. 1. Experimental setup for SHG with LiNbO₃ electro-optic crystal for electric field measurements.



CThD6 Fig. 2. SHG output with respect to external electric field for different pump (≈ 1060 nm) mode conditions.

put with respect to the external electric field. The solid circles show the experimental values, when a predominantly single-mode diode laser was employed. The results were in close agreement with the theoretical estimate (solid line). Higher electric field value (>3 kV/cm) can also be measured by offsetting the initial phase matched condition. The linearity range was calculated to be ≈ 1 kV/cm when the acceptable error was considered to be within 3%. In Fig. 2, the solid squares show the change in the output when a multi-mode diode laser was used. The acceptance bandwidth for the phase matching was considerably broadened due to multi-mode pump laser. This method can also be used for widening the dynamic range of the measurement.

In the experiment, the temperature control of the LiNbO₃ was critical and the acceptance bandwidth was measured to be around 0.8°C FWHM which was in agreement with the theoretical value of 0.7°C . To maintain the stability of the output within 3%, it was necessary to control the temperature within 0.15°C . On the other hand, a KTP (KTiOPO₄) crystal can also be considered for the application, even though the frequency conversion efficiency is lower than the LiNbO₃. It has relatively wide temperature acceptance bandwidth ($\approx 20^\circ\text{C}$) and the temperature control within 4°C is sufficient for the stable output. Figure 3 shows the estimated SHG output corresponding to the external electric field. The mea-



CThD6 Fig. 3. Theoretical estimate of external electrical field by using SHG combined with KTP crystal. Pump wavelength = 1060 nm.

suring range and the linearity range (≈ 2.5 kV/cm) are also wider.

The experimental measurements combined with theoretical estimates show that even though the temperature control is a critical requirement, SHG with electro-optic crystals, such as either LiNbO₃ or KTP, can be effectively used for electrical field measurements.

References

1. Y. Murooka and T. Nakano, "High-sensitive Pockels field sensor with a dielectric mirror," *Rev. Sci. Instrum.* 65, 2351-2355 (1994).
2. A. Yariv, *Quantum Electronics* (John Wiley and Sons, 1989), Chap. 14, 16.
3. V.G. Dimtriev, G.G. Gurzadyan and D.N. Nikogosyan, *Handbook of Nonlinear Optical Crystals* (Springer-Verlag, 1997).

CThD7

9:30 am

Azimuthal Instabilities of Intense Femtosecond Pulses Propagating in Air

S. Skupin, U. Peschel, and F. Lederer, Institut für Festkörpertheorie und Theoretische Optik, Friedrich-Schiller-Universität, 07743 Jena, Germany, Email: stefan@pinet.uni-jena.de

The propagation of intense femtosecond pulses in air and their spatial filamentation has attracted much interest in the past years.¹⁻⁶ In order to understand how rotationally symmetric initial beams change their azimuthal shape, we numerically perform a linear stability analysis.

Our model accounts for dispersive and diffractive broadening as well as for the action of a cubic nonlinearity and of the generated plasma.⁴ The equation for the slowly varying envelope of the electric field $E(x, y, z, \tau)$ in a reference frame moving with the group velocity of the light is given by

$$\partial_z E = i \frac{\Delta_\perp}{2k_0} E - i \frac{k''}{2} \partial_\tau^2 E + i \frac{\omega_0}{c} n_2 |E|^2 E$$

$$E = \frac{\sigma}{2} (1 + i\omega_0 \tau_0) \rho E - \frac{\beta^{(K)}}{2} |E|^{2K-2} E, \quad (1)$$

where ω_0 is the carrier frequency and $k_0 = (\omega_0/c)n$ the propagation constant.

$$k'' = \frac{\partial^2 k}{\partial \omega^2}$$

accounts for the group velocity dispersion and $\rho(x, y, z, \tau)$ for the electron density.

$$\sigma = \frac{\omega_0 \mu_0 e^2 \tau_0}{k_0 m_e (1 + \omega_0^2 \tau_0^2)},$$

τ_0 is the electron collision time and $\beta^{(K)}$ the coefficient of the K -photon absorption. $n_2 |E|^2$ is the refractive index-change, which is induced by the cubic nonlinearity of air. The evolution of the plasma density, which is driven by the K -photon absorption is described by

$$\partial_t \rho = \frac{\beta^{(K)}}{K \hbar \omega_0} |E|^{2K}, \quad (2)$$

where we neglect cascade ionization and electron recombination because of the short pulse duration (for relevant parameters see⁴).